Research Article | Vol. 2, No. 1 | 15 Jan 2019 | OSA CONTINUUM 92
OSA CONTINUUM

Self calibration iso-pathlength point in cylindrical tissue geometry: solution of steady-state photon diffusion based on the extrapolated zero-boundary

HAMOOTAL DUADI,[1] DAQING PIAO,[2,3] AND DROR FIXLER[1,*]

[1]*Faculty of Engineering and the Institute of Nanotechnology and Advanced Materials, Bar Ilan University, Ramat Gan, 5290002, Israel*
[2]*School of Electrical and Computer Engineering, Oklahoma State University, Stillwater, OK 74078, USA*
[3]*Department of Veterinary Clinical Sciences, Center for Veterinary Health Sciences, Oklahoma State University, Stillwater, OK 74078, USA*
**Dror.Fixler@biu.ac.il*

Abstract: Near-infrared optical techniques permit tissue diagnosis by surface measurement. However, the geometrical shape of this interface profiles the intensity of the surface measurement, which is found to have an iso-pathlength (IPL) point allowing for absorption identification independent of tissue scattering. The IPL point was projected in Monte Carlo (MC) simulation, validated experimentally in cylindrical tissues, but remains under-appreciated through analytical approaches. In this work, we present an analytical solution of an IPL point for steady-state diffusion based on the extrapolated zero-boundary condition. The same IPL points were found when comparing this solution to 3-D MC simulations for a tissue radius range of 5-8mm.

1. Introduction

Light-tissue interactions are commonly studied for near infra-red (NIR) spectroscopy for imaging and diagnosis. While imaging is bound to the surface due to the high tissue scattering [1–4], many diagnosis methods, such as the photoplethysmography (PPG) and pulse oximetery, focus on sensing instead of imaging, requiring rapid forward estimation of the surface measurement in response to preferably a homogeneous optical entity of the medium [5,6].

There are two inversion approaches for the investigation of light-tissue interactions: one numerical and the other analytical. The most robust numerical method is the Monte Carlo (MC) simulation [7], which is a study of statistical photon migration based on the optical properties of the different tissue regions. However, the accuracy of such statistical approaches is limited when speed is concerned. Analytical methods based on the diffusion approximation to radiative transfer allow fast forward computation [8]. These methods apply mathematical tools to identify Green functions that fulfill the boundary conditions of the problem in a specific geometry. The common boundary condition of zero fluence rate is set at the tissue-air interface, and two inputs are defined; an isotropic source inside the tissue and an additional image source outside the tissue. The idea is that since photons have an initial direction of entering the tissue normal to the boundary, the diffuse photon propagation in a tissue with a reduced scattering coefficient of μ_s', having units of cm^{-1}, can be attributed to a boundary-affected isotropic source after they scatter and completely lose their memory at $r = R_0\text{-}R_a$ (Fig. 1), where:

$$R_a = 1/\mu_s'. \quad (1)$$

#347794 https://doi.org/10.1364/OSAC.2.000092
Journal © 2019 Received 10 Oct 2018; revised 25 Nov 2018; accepted 25 Nov 2018; published 21 Dec 2018

OSA CONTINUUM

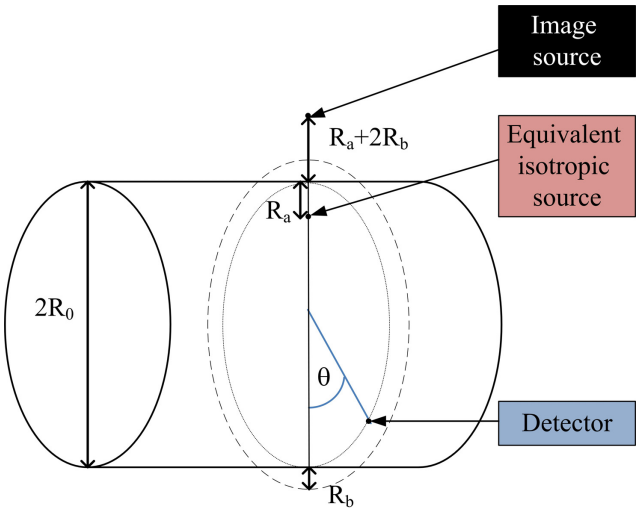

Fig. 1. Details of a cylindrical geometry corresponding to a concave tissue medium. The red arrow indicates the incident light. The positions of the image source, the equivalent isotropic source, and the extrapolated zero-boundary (dashed line) are also illustrated.

In this method, a solution based on Bessel and modified Bessel functions was found for cylindrical geometries [9]. However, a more accurate extrapolated zero-boundary condition yields a solution based on modified Bessel functions of the first and second kind [10–13]. In this paper we will use the solution of steady-state photon diffusion based on the extrapolated zero-boundary and compare it to MC simulations in cylindrical geometry.

2. Solution of steady-state diffusion in cylindrical concave geometry

In the extrapolated zero-boundary condition method, the Fresnel reflection due to the refractive index change on the tissue-detector interface is accounted for by placing the boundary of zero fluence rate away from the physical tissue-air interface. This is accomplished by defining an extrapolated boundary located a distance $R_b = 2A \cdot D$ outside the turbid medium, meaning at $r = R_0 + R_b$ (Fig. 1), where D is the diffusion coefficient to be defined below and A accounts for the effect of the refractive index mismatch as $A = (1 + R_{eff})/(1-R_{eff})$, with R_{eff} being the effective reflection coefficient [14]. The image source, that sets the fluence rate to zero on the extrapolated boundary, is now located at $r = R_0 + R_a + 2R_b$.

In steady-state, photon diffusion in a homogeneous medium is described by [5,6]:

$$\nabla^2\Psi\left(\vec{r}\right)-\frac{\mu_a}{D}\Psi\left(\vec{r}\right)=-\frac{S\left(\vec{r}\right)}{D} \tag{2}$$

where Ψ is the photon fluence rate in units of $W\cdot cm^{-2}$, S is the illumination source intensity in units of $W\cdot cm^{-3}$, μ_a is the absorption coefficient of the tissue, having units of cm^{-1}, and the diffusion coefficient D, having units of cm [15], is defined by μ_a and μ_s' to be:

$$D=\left[3\left(\mu_a+\mu_s'\right)\right]^{-1} \tag{3}$$

Fourier analysis of Eq. (2) derives the Green functions that fulfill the boundary condition. For the cylindrical geometry of the source and detector on the same azimuthal plane as specified in Fig. 1, the following solution to Eq. (2) was found [13]:

OSA CONTINUUM

$$\Psi(\theta)=\frac{S}{2\pi^2 D}\sum_{m=0}^{\infty}\sum_{k} I_m\left[k_{eff}\left(R_0-R_a\right)\right]K_m\left(k_{eff}R_0\right)\cdot\left[1-\frac{I_m\left(k_{eff}R_0\right)K_m\left[k_{eff}\left(R_0+R_b\right)\right]}{K_m\left(k_{eff}R_0\right)I_m\left[k_{eff}\left(R_0+R_b\right)\right]}\right]\cos\left(m\theta\right) \tag{4}$$

where $k_{eff}=\sqrt{k^2+k_0^2}$ is defined and $k_0=\sqrt{\mu_a/D}$ is the effective attenuation coefficient. This azimuthal distribution of the photon fluence rate correlates to the previously defined full scattering profile (FSP) [16].

3. MC simulation of cylindrical geometry

MC simulations revealed that the FSP has a fixed intensity point identified as the iso-pathlength (IPL) point, which does not depend on the reduced scattering coefficient. The location of this point depends solely on the geometry of the tissue-air interface. These findings were validated by tissue mimicking phantoms [17], as well as *in vivo* human finger measurements [18].

The MC simulation is based on the assumption that photons enter the tissue at a certain known direction and interact with the tissue via absorption or scattering processes in accordance to its optical properties. Once the photon enters the tissue interface, its probability to scatter after a distance *dr* is given by:

$$P_{scatter}=1-e^{-\mu'_s dr} \tag{5}$$

Hence, its new direction (θ_{new}) with respect to the immediate previous (old) direction (θ_{old}) is amended by the anisotropy *g*:

$$\theta_{new}=\theta_{old}+\tilde{s}\cdot cos^{-1}\left(g\right) \tag{6}$$

where $\tilde{s}$ is a random number bounded within [-1, 1]. Hence, the subsequent scattering angle is uniformly distributed when the reduced scattering property is concerned. This process is repeated until the photon reencounters the tissue-air interface. The photons' locations in this tissue-air interface assemble the FSP.

OSA CONTINUUM

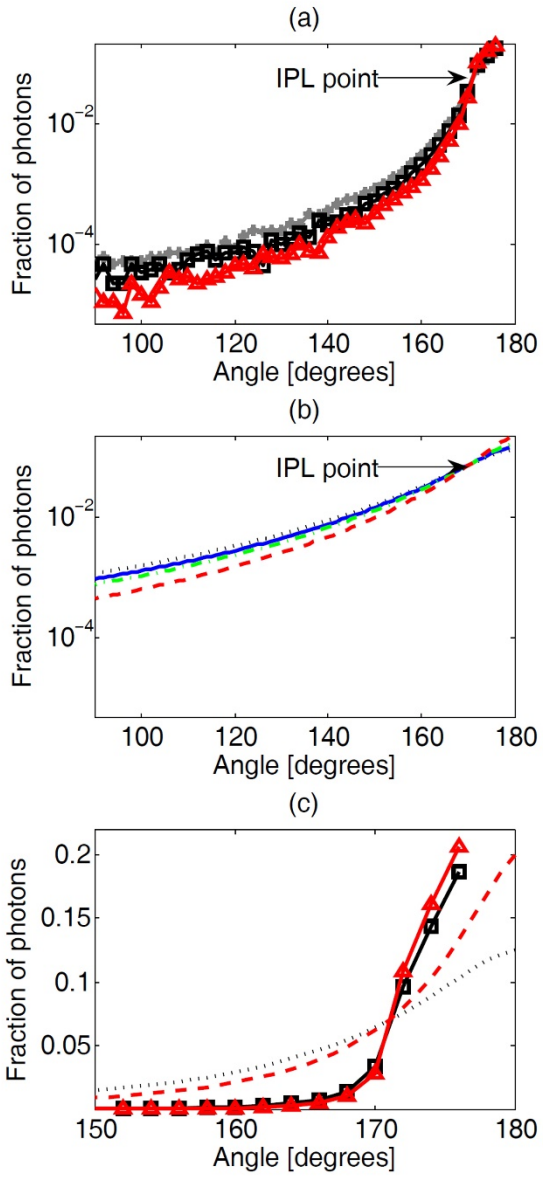

Fig. 2. FSPs and the IPL point resulted from 3-D MC simulation and diffusion theory for steady-state photon illumination into a concave cylindrical tissue domain. Tissue radius is R_0 = 6mm. The FSP has an IPL point which is constant for different reduced scattering coefficients: (a) In the MC simulation gray asterisks, black squares and red triangles correspond respectively to μ_s' = 10, 16 and 26cm^{-1}. (b) In the diffusion theory black dotted, blue solid, green dot-dashed and red dashed lines represent respectively μ_s' = 16, 18, 20 and 26 cm^{-1}. (c) Comparison of 3-D MC simulation and diffusion theory reveals a common IPL point at 171°.

4. IPL point in MC simulation and steady-state diffusion theory

The FSPs of a 6mm radius cylinder was simulated by such a 3-D MC simulation with an absorption coefficient of μ_a = 0.025cm^{-1} and different reduced scattering coefficients. The FSPs from the MC simulations are shown in Fig. 2(a) (gray asterisks, black squares, and red

OSA CONTINUUM

triangles correspond respectively to a reduced scattering coefficient of 10, 16 and 26cm^{-1}). The FSPs reveal an IPL point at 171°.

The FSPs based on the steady-state diffusion theory are developed by assuming a spatially impulse light source injected to the tissue at an initial direction normal to the tissue surface (Eq. (4)), R_{eff} = 0.43, 150 orders of the Bessel and modified Bessel functions (m = 0-150), and 50 k_{eff} values. The results are presented in Fig. 2(b) (black dotted, blue solid, green dot-dashed and red dashed lines represent respectively a reduced scattering coefficient of 16, 18, 20 and 26 cm^{-1}). In the diffusion theory, lower reduced scattering coefficients are less relevant and thus not as accurate since they yield a large transport mean free path (MFP'), which is too far from the light source. Hence, the lowest reduced scattering coefficient was chosen to be 16cm^{-1}, corresponding to MFP' = 0.625mm, in order to maintain an order of magnitude from the radius. The FSPs present an IPL point at an identical position of 171°.

Next, we compare both methods (Fig. 2 (c)). The FSPs of the MC simulation for different reduced scattering coefficients (black squares and red triangles represent respectively a reduced scattering coefficient of 16 and 26 cm^{-1}) are used for examining the FSPs of the diffusion theory (black dotted and red dashed lines represent respectively a reduced scattering coefficient of 16 and 26 cm^{-1}). These two methods, although producing very different FSPs, converge to the same IPL point. The existence of a single point matching IPL over the diverse FSPs from the numerically straightforward method of diffusion theory when compared to the computationally intensive MC method is encouraging.

It is well known that diffusion theory-based solutions are inaccurate near the light source in addition to low scattering condition, when in comparison to the more precise MC methods. The inaccuracy of the diffusion-based solution presented in Eq. (4) at a near-the-entry distance is also apparent from the IPL point's location in various tissue radiuses (Fig. 3). A comparison between MC simulation and diffusion theory (red circles and blue squares in Fig. 3) reveals this divergence in the low radius range since the IPL point is too close to the source. A recent work has demonstrated a simple approach to enhancing the diffusion-based estimation of the photon fluence rate at distances near the point-of-entry for surface measurement [19]. That approach, when extended to the analysis of the FSP in cylindrical geometry, is expected to enhance the match between analytical prediction and MC measurement of the IPL.

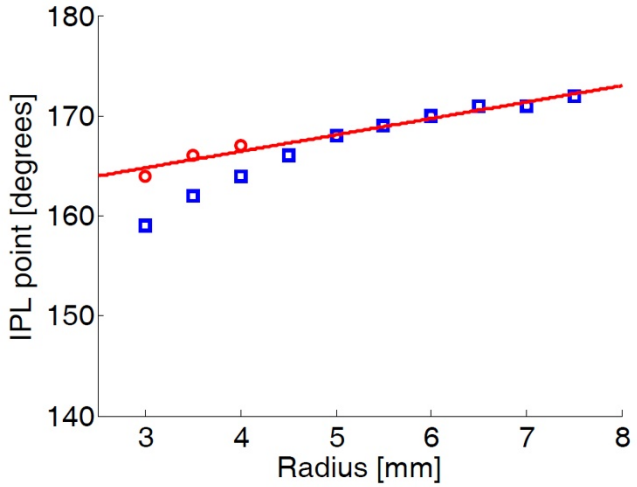

Fig. 3. The influence of radius on the IPL point. IPL point from MC simulation (red circles, STD = ± 1°) and from diffusion theory (blue squares, STD = ± 0.5°).

OSA CONTINUUM

5. Discussion and conclusions

In real-time sensing applications, the reading from sensors implemented with IPL principles may be conducted when the sensor concave geometries change in adapting to tissue-air interface. In such situations, any change of the sensor geometry, in terms of the radius of the concave shape, must be accounted for rapidly for accurate inversion of the tissue optical properties. Analytical knowledge of the IPL point will be important for real-time IPL-based identification of tissue absorption properties for cylindrical tissue geometries.

For endoscopic applications involving a convex tissue geometry that can be simplified by a cylinder of air surrounded by tissue of homogeneous properties, the solution of photon diffusion as a counterpart of Eq. (4) is the following:

$$\Psi(\theta)=\frac{S}{2\pi^2 D}\sum_{m=0}^{\infty}\sum_{k} I_m\left[k_{eff}R_0\right]K_m\left(k_{eff}\left(R_0+R_a\right)\right)\cdot\left[1-\frac{K_m\left(k_{eff}R_0\right)I_m\left[k_{eff}\left(R_0-R_b\right)\right]}{I_m\left(k_{eff}R_0\right)K_m\left[k_{eff}\left(R_0-R_b\right)\right]}\right]\cos\left(m\theta\right) \tag{7}$$

A simulation of the FSPs for the convex geometry (Fig. 4) presents results similar to that in a concave geometry of the same radius (Fig. 2). This finding was expected, since we have projected in the past that the IPL point phenomena in different geometries can be predicted by the distance between the light source and the detector [20]. The simulation results will encourage further experimental studies of IPL behaviors in such a convex geometry, both in MC simulation and using phantom materials, for gauging the solution of steady steady-state photon diffusion.

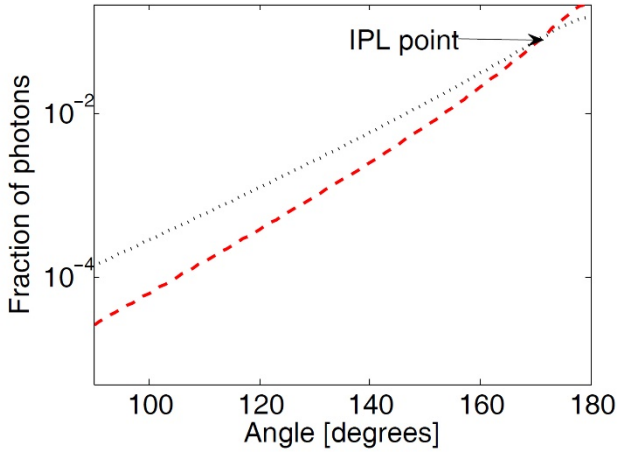

Fig. 4. The FSPs of steady-state photon diffusion for a convex geometry with a radius of 6mm, where a cylinder of air is surrounded by tissue (Eq. (7). Different reduced scattering coefficients (μ_s' = 16 and 26 cm^{-1} corresponding to black dotted and red dashed lines) have a common IPL point at 171°.

Furthermore, the geometry where the source and detector are not on the same azimuthal plane is also possible. The evaluation of the IPL point along the longitudinal direction should be investigated as well.

The comparison of the IPL points given by MC and by diffusion theory for the longitudinal direction, whether that will give the same IPL points comparing to the presented azimuthal directions or not, could give additional support to this work.

To conclude, in this study we derived the FSP from the steady-state diffusion theory based on the extrapolated zero-boundary condition. A comparison of different reduced scattering

OSA CONTINUUM

coefficients revealed the IPL point, where the intensity remains constant regardless of the scattering property of the tissue. The position of the IPL according to this theoretical method is in agreement with the MC simulations performed under the same geometrical parameters and optical properties [21,22].

References

1. K. P. Nadeau, T. B. Rice, A. J. Durkin, and B. J. Tromberg, "Multifrequency synthesis and extraction using square wave projection patterns for quantitative tissue imaging," J. Biomed. Opt. **20**(11), 116005 (2015).
2. V. Ntziachristos, "Going deeper than microscopy: the optical imaging frontier in biology," Nat. Methods **7**(8), 603–614 (2010).
3. V. V. Tuchin, *Optical clearing of tissues and blood* (SPIE Press, Bellingham, WA, 2006).
4. T. D. O'Sullivan, A. E. Cerussi, D. J. Cuccia, and B. J. Tromberg, "Diffuse optical imaging using spatially and temporally modulated light," J. Biomed. Opt. **17**(7), 071311 (2012).
5. O. Wieben, in *Design of Pulse Oximeters*, edited by J.G. Webster (Taylor & Francis, 1997), p. 40–55.
6. J. T. B. Moyle, in *Pulse Oximetry* (BMJ Books London, 2002).
7. L. Wang, S. L. Jacques, and L. Zheng, "MCML--Monte Carlo modeling of light transport in multi-layered tissues," Comput. Methods Programs Biomed. **47**(2), 131–146 (1995).
8. S. L. Jacques and B. W. Pogue, "Tutorial on diffuse light transport," J. Biomed. Opt. **13**(4), 041302 (2008).
9. S. R. Arridge, M. Cope, and D. T. Delpy, "The theoretical basis for the determination of optical pathlengths in tissue: temporal and frequency analysis," Phys. Med. Biol. **37**(7), 1531–1560 (1992).
10. B. W. Pogue and M. S. Patterson, "Frequency-domain optical absorption spectroscopy of finite tissue volumes using diffusion theory," Phys. Med. Biol. **39**(7), 1157–1180 (1994).
11. A. Sassaroli, F. Martelli, G. Zaccanti, and Y. Yamada, "Performance of fitting procedures in curved geometry for retrieval of the optical properties of tissue from time-resolved measurements," Appl. Opt. **40**(1), 185–197 (2001).
12. D. Piao, R. L. Barbour, H. L. Graber, and D. C. Lee, "On the geometry dependence of differential pathlength factor for near-infrared spectroscopy. I. Steady-state with homogeneous medium," J. Biomed. Opt. **20**(10), 105005 (2015).
13. A. Zhang, D. Piao, C. F. Bunting, and B. W. Pogue, "Photon diffusion in a homogeneous medium bounded externally or internally by an infinitely long circular cylindrical applicator. I. Steady-state theory," J. Opt. Soc. Am. A **27**(3), 648–662 (2010).
14. R. C. Haskell, L. O. Svaasand, T. T. Tsay, T. C. Feng, M. S. McAdams, and B. J. Tromberg, "Boundary conditions for the diffusion equation in radiative transfer," J. Opt. Soc. Am. A **11**(10), 2727–2741 (1994).
15. R. Graaff and J. J. Ten Bosch, "Diffusion coefficient in photon diffusion theory," Opt. Lett. **25**(1), 43–45 (2000).
16. H. Duadi, I. Feder, and D. Fixler, "Linear dependency of full scattering profile isobaric point on tissue diameter," J. Biomed. Opt. **19**(2), 026007 (2014).
17. I. Feder, H. Duadi, and D. Fixler, "Experimental system for measuring the full scattering profile of circular phantoms," Biomed. Opt. Express **6**(8), 2877–2886 (2015).
18. H. Duadi, I. Feder and D. Fixler, "Near-infrared human finger measurements based on self-calibration point: Simulation and in vivo experiments," J. Biophot. 11 (2018)
19. D. Piao and S. G. Patel, "A simple empirical master-slave dual-source configuration within the diffusion approximation enhances modeling of spatially resolved diffuse reflectance at short-path and with low-scattering from a semi-infinite homogeneous medium," Appl. Opt. **56**(5), 1447–1452 (2017).
20. I. Feder, H. Duadi, R. Chakraborty, and D. Fixler, "Self-Calibration Phenomenon for Near-Infrared Clinical Measurements: Theory, Simulation, and Experiments," ACS Omega **3**(3), 2837–2844 (2018).
21. D. Fixler, J. Garcia, Z. Zalevsky, A. Weiss, and M. Deutsch, "Speckle random coding for 2D super resolving fluorescent microscopic imaging," Micron **38**(2), 121–128 (2007).
22. D Fixler, Y Namer, Y Yishay, and M. Deutsch, "Influence of fluorescence anisotropy on fluorescence intensity and lifetime measurement: theory, simulations and experiments," IEEE Trans. Biomed. Eng. **53**(6), 1141–1152 (2006).